1-D Analysis of the Plasma Plume of a Hollow Cathode with Magnetic Nozzle

Merugu Divyasimha

Aerospace Division, Dept. of Civil and Industrial Engineering, University of Pisa, Italy
d.merugu@studenti.unipi.it

Abstract

A one-dimensional (1-D) model for the study of the plasma plume generated by the hollow cathode with a magnetic nozzle has been developed. The fluid equations of the model have been solved numerically, under the assumptions of an axial magnetic field and that all the parameters vary only in the axial direction. The plasma is assumed to be quasi-neutral. The variation of the plasma parameters as the plasma expands in the magnetic nozzle has been investigated for a xenon mass flowrate of 1.5 mg/s, 30 A of current and 50 mT of maximum applied magnetic field. In the energy equation for ions and neutrals, heat flow and thermal conductivity have been considered low and hence neglected. Finally, thrust using the magnetic nozzle has been computed and compared with the thrust without magnetic nozzle, finding that the application of the magnetic field allows for significantly higher thrust production.

Nomenclature

B_z = magnetic field in z direction [T]

$\dot{m}$ = mass flow rate [mgs^{-1}]

m_e= mass of electron [kg]

m_i = mass of ion [kg]

n_e = number density of electron, m^{-3}

n_i = number density of ion, [m^{-3}]

n_n = number density of neutrals, m^{-3}

$u_{e\varphi}$ = azimuthal velocity [m/s]

μ_O = permeability of free space

A_k = Keeper Area, m^2

A = area of the flux tube

B = magnetic field [T]

e = charge of electron 1.60217662*10^{-19} C

I = current [A]

N = number of turns of solenoid

R_c = radius of the solenoid

r = radius of the flux tube

U = first ionization energy of Xenon [V]

γ = specific heat ratio

T_e = electron temperature, K

T_i = T_n = ion and neutral temperature, K

u_{ez} = electron axial velocity u_{iz} = ion axial velocity [m/s]

u_{nz} = neutral axial velocity [m/s]

ν_{ei} = electron-ion collision frequency

ν_{en} = electron-ion collision frequency

K = Boltzmann constant,1.38064852 × 10^{-23} m^2 kg s^{-2} K^{-1}

S = collision cross-section

Φ = potential [V]

E = electric field

P = pressure

I. INTRODUCTION

Hollow cathodes (HC) are extensively used space devices with application in electric propulsion as electron sources for discharge and neutralization in Hall Effect Thrusters (HET) and Gridded Ion Thrusters. The operation of the HC is based on field-enhanced thermionic electron emission from an insert inside the body of the cathode. Electrons are drawn to an external electrode (anode) which is kept at voltages slightly higher than the ionization potential of the operating gas. HC's operate at temperatures of over 1600 K, thus they are typically made of refractory metals.

Hollow Cathode Working: Figure 1 [4] is a schematic representation of a HC. A thin, orificed tube made up of refractory material is fed with the propellant; the "emitter" (or "insert") is placed inside the tube in contact with the orifice by means of a spring spacer system. The emitter is a hollow cylinder made up of a low work function material which provides electrons through field enhanced thermionic effect. A "keeper" electrode is kept at a positive potential with respect to cathode. The electrons which are emitted from the emitter will accelerate towards the keeper electrode which causes the ionization of the propellant and the creation of a plasma. This keeper electrode is wrapped around the cathode tube with an insulation (ceramic wall) between them [2].

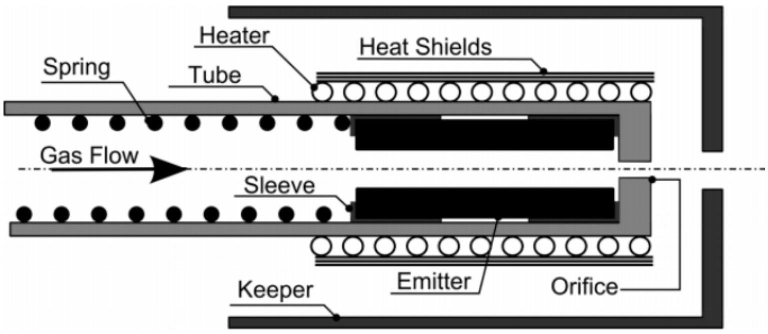

Figure 1 - General schematic of an orificed hollow cathode.

Hollow cathodes may represent an attractive propulsion device for a number of reasons. Spacecraft which operate primary electrostatic or electromagnetic propulsion systems such as gridded ion thrusters and Hall thrusters are typically required to carry a secondary chemical system for reaction/momentum control or to compensate for thrust misalignment. In the stand-alone configuration, the hollow cathodes are able to produce a decent amount of thrust required to perform these maneuvers for small satellites depending on the operating conditions [5]. In this paper a magnetic nozzle configuration is chosen for the hollow cathode (Fig. 1.1) and the detailed analysis is carried on checking whether the magnetic nozzle enhanced the performance of the cathode in terms of thrust production when compared to stand-alone configuration without magnetic nozzle. The main advantage of using the magnetic nozzle is the capability to change the strength and geometry of the applied magnetic field in flight allowing the nozzle to adapt to different propulsive requirements. The magnetic nozzle in Figure 1.1 is created with a solenoid and placed in such a way that the field is at a maximum at the throat of the keeper.

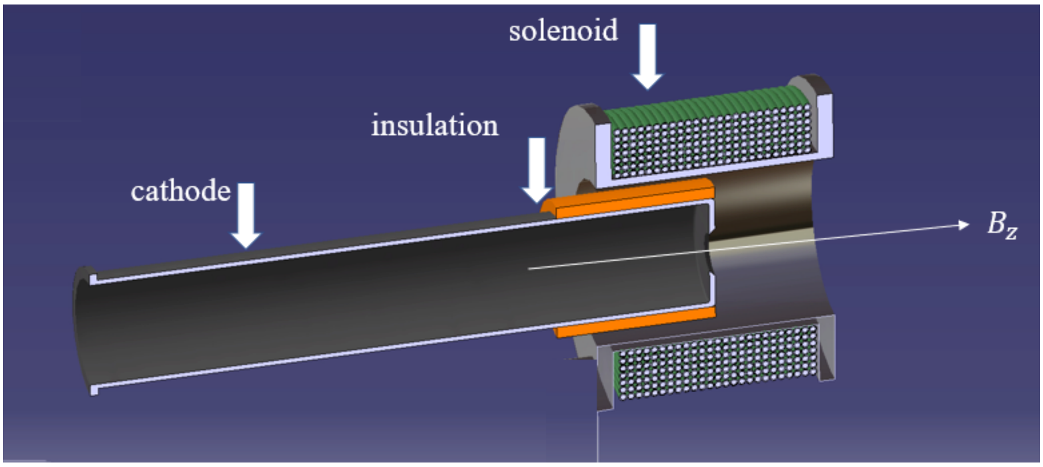

Figure 1.1 - General schematic of a hollow cathode with a magnetic nozzle downstream of the cathode.

A detailed explanation of the working and thrust production mechanism of the cathode with the magnetic nozzle is presented in section **2**. In section **3** and **4** a brief description of the solenoid magnetic field topology and how the plasma is confined and expanded with the diverging field is reported. Section **5** addresses the problem in terms of plasma fluid equations in the divergence form and then in section **6** the equations are resolved, under proper assumptions, in a cylindrical coordinate system which is suitable to our geometry. Section **7** and **8** describes how the equations are numerically solved. Finally, in section **9** the simulation results are presented with a comparison between the two cathode configurations, respectively with and without magnetic nozzle.

II. MAGNETIC NOZZLE

Magnetic nozzles are functionally similar to De Laval nozzles. They achieve thrust by converting non-directional kinetic energy to directed kinetic energy like in a gas dynamic nozzle where the gas internal energy is converted into axial kinetic energy. [1]

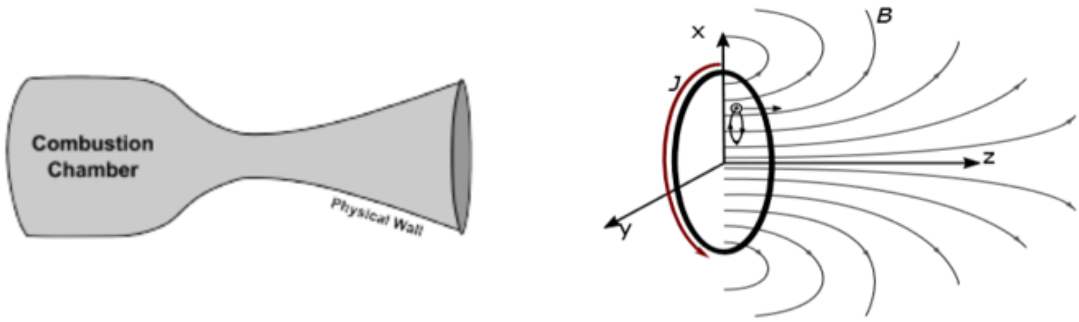

Figure 2.1 - De Laval nozzle compared to magnetic nozzle produced by current loop with current J [8].

Operating Principle:

a) *Conservation of adiabatic invariant (orbital magnetic moment)* $v_\perp \rightarrow v_{||}$

The magnetic moment of a particle $\mu_m = \frac{mv_\perp^2}{2B}$ is an adiabatic constant of motion. The conditions for adiabaticity may be represented by the relations shown in Equation 1.

$$r_L \left|\frac{\nabla B}{B}\right| \ll 1 \qquad (2.1)$$

Due to the spatial variation of magnetic field (eq.1) within in the particle orbit which is much less than compared to the magnitude of B there is a gradual drift of guiding center (*transverse drift velocity)* across **B** and a gradual change of its velocity (*parallel acceleration*) along **B**.

As shown in Figure 2.2, the parallel gradient of the magnetic field acts on the particle as a force which pushes the magnetized electrons downstream [6].

$$\langle F_{||}\rangle = -|\mu|(\nabla B)_{||} \qquad (2.2)$$

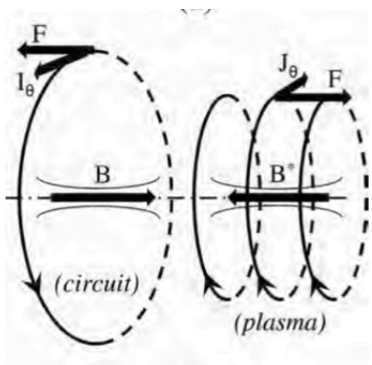

Figure 2.2 - Repulsive force between the induced and the applied magnetic field [2].

Energy exchange

As a consequence of the adiabatic invariance of $|\mu_m|$ and the conservation of the total particle energy, as the particle moves into a region of diverging magnetic field lines (Fig. 1.2) its transverse kinetic energy $W\perp$ decreases, while its parallel kinetic energy $W_{||}$ increases [6].

To describe adiabatic energy exchange, we can use the conservation of total kinetic energy (Eq. 2.3):

$$K_{total} = K_{\perp} + K_{||} = \frac{mv_{\perp}^2}{2} + \frac{mv_{||}^2}{2} = constant \qquad (2.3)$$

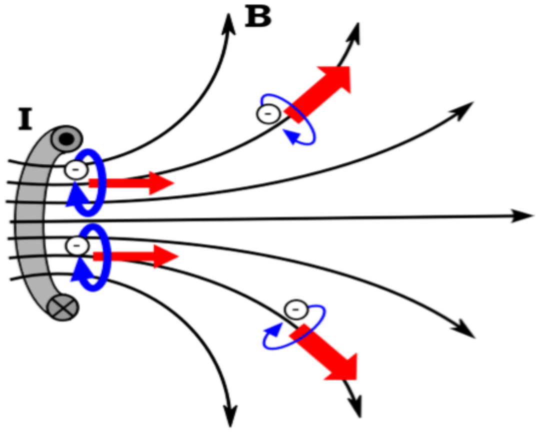

Figure 2.3 - Blue arrows are perpendicular velocities while red arrows are parallel velocities. Thickness of the arrows represents the magnitude of the velocity. [3]

b) *Electric Field Acceleration*

Electric field acceleration may be driven by the formation of ambipolar fields. This mechanism is a result of the high mobility of electrons compared to ions. In expanding magnetic nozzles, the mobile electrons establish an electron pressure gradient ahead of the slow ions. To maintain quasi-neutrality an electric field (fig.3) is established which accelerates ions.

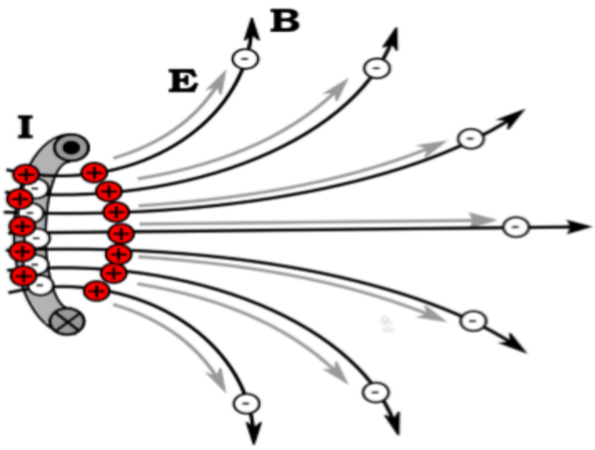

Figure 2.4 - Electric field due to charge imbalance [3].

III. Magnetic field of a solenoid

A solenoid (Fig. 3.1) is used to create the magnetic nozzle for the cathode. The magnetic field inside the solenoid is essentially uniform and is directed along the axis of the solenoid; outside of the solenoid, as we move axially the magnetic field gets weaker and is given by Eq. 3.1. Fig. 3.1 (left) shows the magnetic field topology of the solenoid.

B(z) = $\frac{\mu_0 I R_c{}^2 N}{2\left(R_c{}^2+z^2\right)^{3/2}}$; I = 10 [A]; μ_0 = $1.25664 \times 10^{-6}(T.m/A)$; R_c = 20 [mm] (3.1)

B(max) = $\frac{\mu_0 I N}{2R}$ Maximum magnetic field at center (3.2)

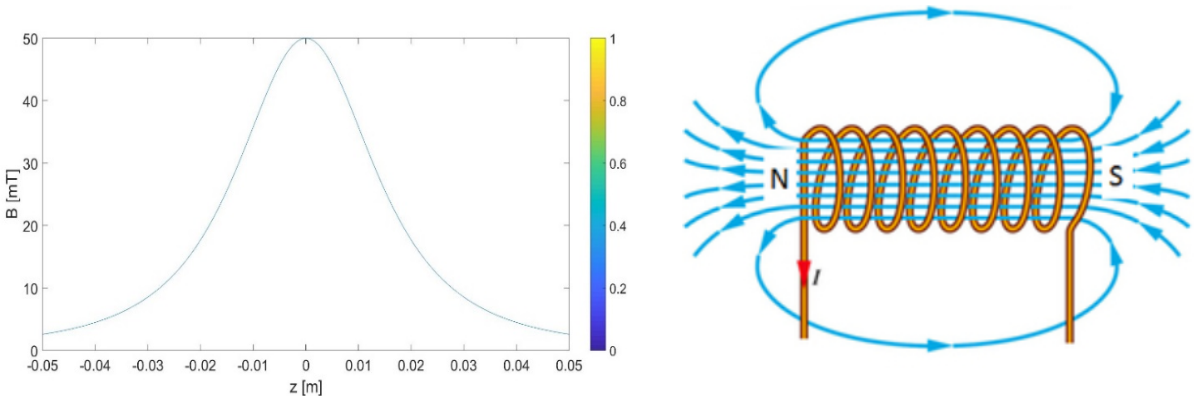

Figure 3.1 - Magnetic field topology of a solenoid.

IV. Cross-sectional Area Variation

The electrons move much faster than ions and a net charge separation occurs which results in the formation of an electric field. The ions are assumed to be non-magnetized and will be accelerated by this electric field. The expansion of the plasma is governed by the magnetic field divergence. The magnetic field bounds the plasma with a magnetic flux surface as shown in Figure 3.1. The cross section of this flux can be approximated using the Gauss law of magnetism:

$$\nabla \cdot B = 0;\ \oiint B.ds = 0 \qquad (4.1)$$

$$\mathrm{A}_z = \frac{B_{z,k}}{B_z}\,\mathrm{A}_k\ ;\ r(z) = \sqrt{\frac{B_{z,t}}{\pi B_z}\,\mathrm{A}_k} \qquad (4.2)$$

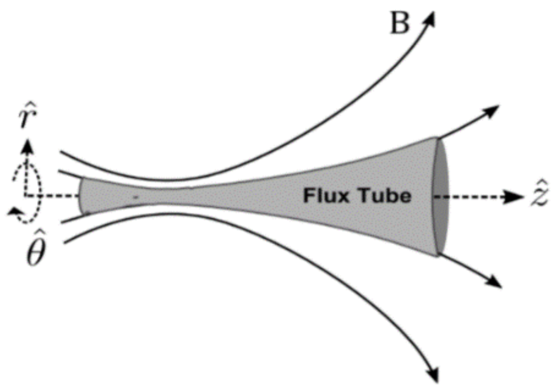

Figure 4.1 - Flux-tube cross sectional area variation.

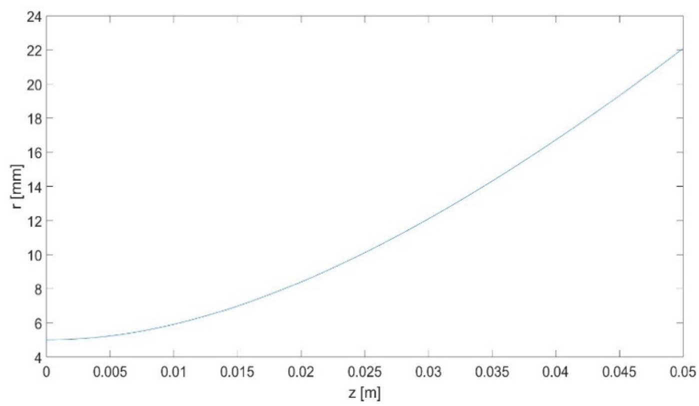

Figure 4.2 - Radius of the magnetic flux tube vs. *z*.

V. Plasma Fluid Equations

Particle conservation

Conservation of particles and charges in the plasma is described by the continuity equation [7]:

$$\frac{\partial n_\alpha}{\partial t} + \nabla \cdot (n_\alpha u_\alpha) = \dot{n_\alpha} \qquad (a)$$

where $\dot{n_\alpha}$ represents the rate per unit volume at which particles of type α ions or electrons produced or lost as a result of collisions.

Momentum conservation

In constructing a fluid approach to plasmas, the three dominant forces on the charged particles in the plasma that transfer momentum that are considered. (1) charged particles react to electric and magnetic field by means of the Lorentz force, (2) the pressure gradient force, (3) collisions transfer momentum between the different charged particles, and also between the charged particles and the neutral gas [7].

$$m_\alpha n_\alpha \left(\frac{\partial u_\alpha}{\partial t} + (u_\alpha \cdot \nabla) u_\alpha\right) + \dot{n_\alpha} m_\alpha u_\alpha = q n_\alpha (E + u_\alpha \times \mathbf{B}) - \nabla P_\alpha - \sum_{\alpha,\beta} m_\alpha n_\alpha \nu_{\alpha\beta} (u_\alpha - u_\beta) \qquad (b)$$

where $\nu_{\alpha\beta}$ represents the collision frequency between species α and β.

Energy conservation

$$\frac{\partial}{\partial t}\left(n_\alpha m_\alpha \frac{{u_\alpha}^2}{2} + \frac{3}{2} P_\alpha\right) + \nabla \cdot \left(n_\alpha m_\alpha \frac{{u_\alpha}^2}{2} + \frac{5}{2} P_\alpha\right) u_\alpha$$
$$= -\nabla \cdot (K \nabla T_\alpha) + q_\alpha n_\alpha E u_\alpha - \sum_{\alpha,\beta} m_\alpha n_\alpha \nu_{\alpha\beta} (u_\alpha - u_\beta) u_\alpha - \Psi_\alpha \qquad (c)$$

The divergence terms on the left-hand side represent the total energy flux and the terms on the right-hand side represents the work done by the electric field force and the collisional force [5].

In the above equation, $\Psi_\alpha = e\dot{n_\alpha} U_i$ represents the electron energy loss due to ionization, with U_i in volts representing the first ionization potential of the atom and pressure term $P_\alpha = nkT_\alpha$.

We made the following assumptions:

- Quasi neutral plasma $n_i = n_e = n$
- steady-state $\frac{\partial}{\partial t} = 0$
- axially symmetric $\frac{\partial}{\partial \varphi} = 0$
- magnetic field $B = B_z \hat{z} + B_r \hat{r}$
- Ions not magnetized
- negligible inertia of electrons
- collisions electron-ion / electron-neutral
- $u_e = u_{ez} \hat{z} + u_{er} \hat{r} + u_{e\varphi} \hat{\varphi}$
- $u_i = u_{iz} \hat{z} + u_{ir} \hat{r}, \ \frac{\partial u_{iz}}{\partial r} = 0$
- $u_n = u_{nz} \hat{z} + u_{nr} \hat{r}, \ \frac{\partial u_{nz}}{\partial r} = 0$

VI. Equations in cylindrical coordinate system

The fluid equation presented above are further reduced to one-dimensional equations in cylindrical coordinates along the *z* component for electron, ion, neutral, with the assumptions stated above.

Equations for electron in 'r, φ, z' component:

Continuity:

$$n \frac{\partial u_{ez}}{\partial z} + \frac{n u_{er}}{r} + u_{ez} \frac{\partial n}{\partial z} = \dot{n}$$

Momentum:

r: $-\dot{n} m_e u_{er} - -enu_\varphi B_z + m_e n \nu_{ei} (u_{ir} - u_{er}) + m_e n \nu_{en} (u_{nr} - u_{er}) = 0$

φ: $-\dot{n} m_e u_{e\varphi} - enu_{ez} B_r - enu_{er} B_z - m_e n \nu_e (u_\varphi) = 0$

z: $-\dot{n}m_e u_{ez} - enE_z - enu_\varphi B_r - \frac{\partial P_z}{\partial z} + m_e n\nu_{ei}(u_{iz} - u_{ez}) + m_e n\nu_{en}(u_{nz} - u_{ez}) = 0$

$$B_r = \frac{-1}{2} r \frac{\partial B_z}{\partial z} \quad and\ r = \frac{u_\varphi}{\Omega}\ ;\ where\ \Omega = \frac{qB}{m}$$

$$B_r = \frac{-1}{2} \frac{u_\varphi m}{q\mathbf{B}} \frac{\partial B_z}{\partial z}$$

z:$-Snn_n m_e u_{ez} - enE_z + n\frac{mu_\varphi{}^2}{2\mathbf{B}}\frac{\partial B_z}{\partial z} - kn\frac{\partial T_e}{\partial z} - kT_e\frac{\partial n}{\partial z} + m_e n\nu_{ei}(u_{iz} - u_{ez}) +$
$m_e n\nu_{en}(u_{nz} - u_{ez}) = 0$

The azimuthal $u_{e\varphi}$ in the momentum equation can be obtained from "r" component of the electron momentum equation:

$$u_{e\varphi} = \frac{-Snn_n m_e u_{er}}{enB_z} - \frac{m_e u_{er}}{eB_z}(\nu_{ei} + \nu_{en})$$

Energy:

z: $\frac{5}{2}nkT_e\frac{\partial u_{ez}}{\partial z} + \frac{5}{2}nk\left(u_{er}\frac{\partial T_e}{\partial r} + u_{ez}\frac{\partial T_e}{\partial z}\right) + \frac{5}{2}kT_e\left(u_{er}\frac{\partial n}{\partial r} + u_{ez}\frac{\partial n}{\partial z}\right) = -n_e u_e eE_z -$
$e\dot{n}_e U_i - Snn_n m_e\frac{u_e{}^2}{2}$

Equations for ion in 'z' component:

Continuity:

$$n\frac{\partial u_{iz}}{\partial z} + \frac{nu_{ir}}{r} + u_{iz}\frac{\partial n}{\partial z} = \dot{n}$$

Momentum:

z: $m_i n\left(u_{iz}\frac{\partial u_{iz}}{\partial z}\right) = -Snn_n m_i u_{iz} + enE_z - kn\frac{\partial T_i}{\partial z} - kT_i\frac{\partial n}{\partial z} - m_e n\nu_{ei}(u_{iz} - u_{ez})$

Energy (from equation of state):

$$\frac{1}{T_i}\frac{\partial T_i}{\partial z} = \frac{\gamma - 1}{n}\frac{\partial n}{\partial z}$$

Equations for the neutrals are same as for the ions but without the electric field terms.

VII. Initial Conditions

From section II we have a set of nine differential equations; to solve them numerically we need nine initial conditions. Such conditions are found from the operating conditions of the cathode at 1.5 mg/s mass flow-rate, I = 30 A keeper current and from the keeper geometry and dimensions. The ions and neutrals are assumed to be initially at same temperature and to have the same velocity (sonic).

1. $\Phi(0) = 20\ [V]$
2. $n(0) = 10^{20}\ m^{-3}$ initial number density for ion-electron
3. $u_{iz}(0) = \sqrt{\gamma RT_i}$ the ion and neutral assumed to have sonic velocity at the keeper
4. $T_i(0) = 3000\ k$ initial temperature for ion-neutral
5. $n_n(0) = \frac{\dot{m} - Au_{iz}(0)m_0 n(0)}{Au_{nz}(0)m_0}$ the initial number density for neutral is found from the continuity equation at inlet and keeper exit using the mass flow-rate 2 mg/s and the keeper dimensions
6. $u_{nz}(0) = u_{iz}(0)$
7. $T_n = T_i$
8. $u_{ez}(0) = \frac{I}{Ane}$ the initial electron drift velocity is found using the keeper current and the keeper dimensions
9. $T_e(0) = 3\ eV$

The radial velocities for electron ion and neutral are assigned as thermal velocities: $u_r = \sqrt{\frac{kT}{m}}$.

VIII. Solving Numerically

From section II we have a set of 9 differential equations with 9 unknowns. In order to solve them numerically using MATLAB these equations are modified in such a form that all the variables or the unknowns which vary along 'z' (independent variable) are functions of all the variables. Mathematically they are reduced to $\frac{dy(i)}{dz} = f(y)$: here 'y(i)' indicates the specific variable of all 9 variables.

$$\frac{\partial\Phi}{\partial z} = \left(\frac{1}{\frac{3}{5} + \frac{kT_e}{\gamma kT_i - m_i u_{iz}^2}}\right)\left[\frac{4Sn_n m_e u_{ez}}{5e} - \frac{Sn_n kT_e}{eu_{ez}} + \frac{kT_e u_{er}}{reu_{ez}} - \frac{2Sn_n U_{ion}}{5u_{ez}} + \frac{m_i u_{iz} u_{ir} kT_e}{er(\gamma kT_i - m_i u_{iz}^2)} - \frac{2m_i kT_e Sn_n u_{iz}}{e(\gamma kT_i - m_i u_{iz}^2)} - m_e n\nu_{ei}(u_{iz} - u_{ez}) - m_e n\nu_{en}(u_{nz} - u_{ez}) - \frac{nmu_\varphi^2}{2B}\frac{\partial B_z}{\partial z}\right] \tag{8.1}$$

$$\frac{\partial n}{\partial z} = \left[\frac{1}{\gamma kT_i - m_i u_{iz}^2}\right]\left(-2m_i u_{iz} Snn_n + \frac{m_i n u_{iz} u_{ir}}{r} - ne\frac{\partial\Phi}{\partial z} - m_e n\nu_{ei}(u_{iz} - u_{ez})\right) \tag{8.2}$$

$$\frac{\partial u_{iz}}{\partial z} = Sn_n - \frac{u_{ir}}{r} - \frac{u_{iz}}{n}\frac{\partial n}{\partial z} \tag{8.3}$$

$$\frac{\partial T_i}{\partial z} = \frac{T_i(\gamma - 1)}{n}\left[\frac{1}{\gamma kT_i - m_i u_{iz}^2}\right]\left(-2m_i u_{iz} Snn_n + \frac{m_i n u_{iz} u_{ir}}{r} - ne\frac{\partial\Phi}{\partial z} - m_e n\nu_{ei}(u_{iz} - u_{ez})\right) \tag{8.4}$$

$$\frac{\partial u_{ez}}{\partial z} = Sn_n - \frac{u_{ir}}{r} - \frac{u_{ez}}{n}\left[\frac{1}{\gamma kT_i - m_i u_{iz}^2}\right]\left(-2m_i u_{iz} Snn_n + \frac{m_i n u_{iz} u_{ir}}{r} - ne\frac{\partial\Phi}{\partial z} - m_e n\nu_{ei}(u_{iz} - u_{ez})\right) \tag{8.5}$$

$$\frac{\partial T_e}{\partial z} = \frac{-Sn_n T_e}{u_{ez}} + \frac{T_e u_{er}}{ru_{ez}} + \frac{2e}{5k}\frac{\partial\Phi}{\partial z} - \frac{2eSn_n U_{ion}}{ku_{ez}} - \frac{Sn_n m_e u_{ez}}{5k} \tag{8.6}$$

$$\frac{\partial n_n}{\partial z} = \left[\frac{1}{1 - \frac{m_n u_{nz}^2}{kT_n}}\right]\left(2\frac{Snn_n m_n u_{nz}}{kT_n} + \frac{m_n n_n u_{nz}}{kT_n}\left[\frac{u_{nr}}{r}\right] - \frac{n_n}{T_n}\frac{\partial T_n}{\partial z} - \frac{m_e n\nu_{en}(u_{nz} - u_{ez})}{kT_n}\right) \tag{8.7}$$

$$\frac{\partial u_{nz}}{\partial z} = -\frac{\dot{n}}{n_n} - \frac{u_{nr}}{r} - \frac{u_{nz}}{n_n}\frac{\partial n_n}{\partial z} \tag{8.8}$$

$$\frac{\partial T_n}{\partial z} = T_n\frac{\gamma - 1}{n_n}\left[\frac{1}{1 - \frac{m_n u_{nz}^2}{kT_n}}\right]\left(2\frac{Snn_n m_n u_{nz}}{kT_n} + \frac{m_n n_n u_{nz}}{kT_n}\left[\frac{u_{nr}}{r}\right] - \frac{n_n}{T_n}\frac{\partial T_n}{\partial z} - \frac{m_e n\nu_{en}(u_{nz} - u_{ez})}{kT_n}\right) \tag{8.9}$$

IX. Results

Solving numerically the above discussed equations with the initial conditions presented in the section VII yields results which are shown in this section, also a comparison was made for all the variation of all the 9 variables with two cases.

Case 1. Magnetic Field B = 0

Case 2. Magnetic Field B = 50 [mT]

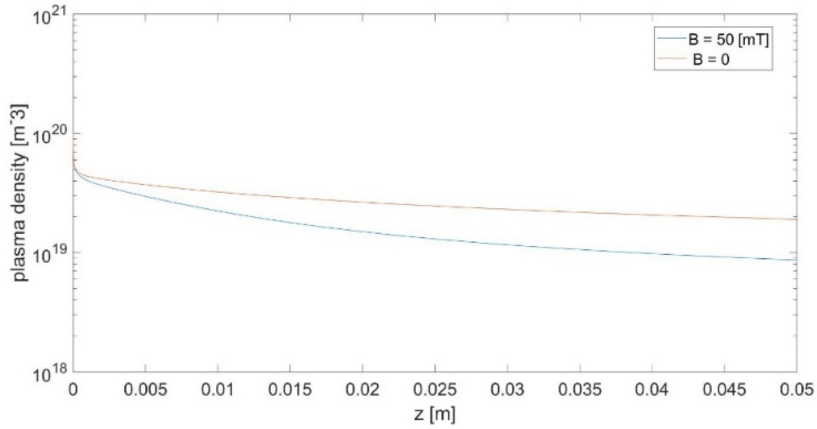

Figure 9.1 **-** Plasma density as a function of distance from the cathode.

The plasma density as it expands into the vacuum with the magnetic function field is compared without Magnetic nozzle, it can be seen that the number density decreases as we move away from the cathode which is expected.

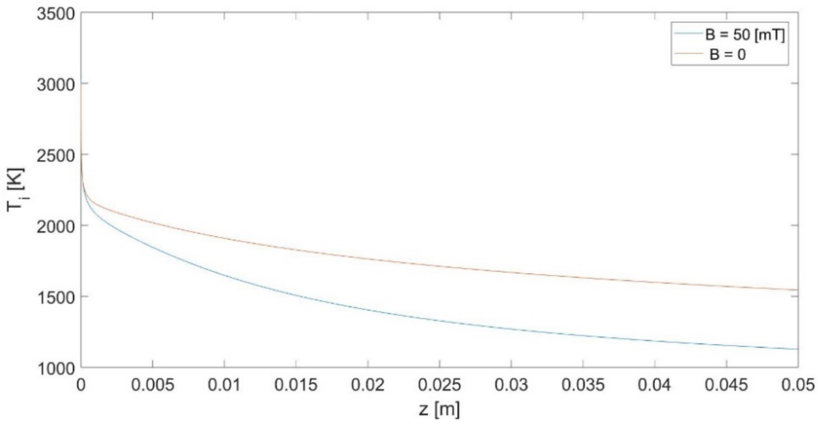

Figure 9.2 - Ion Temperature [K].

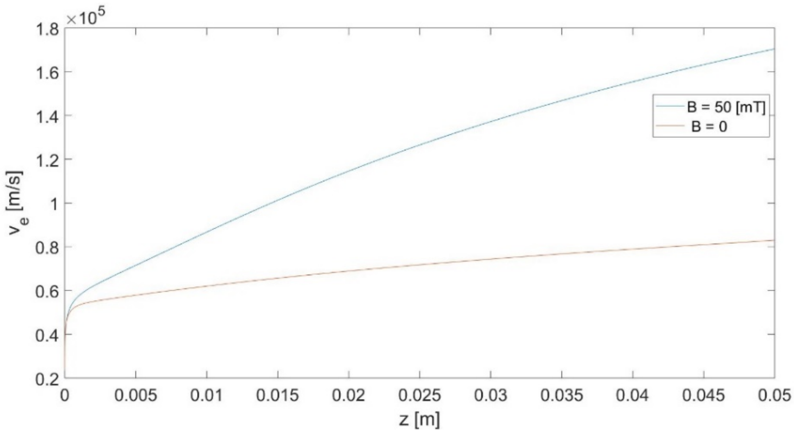

Figure 9.3 - Electron velocity [m/s].

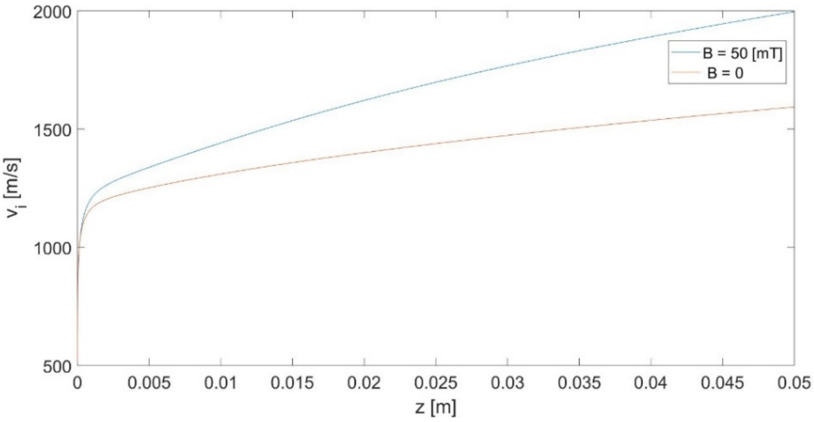

Figure 9.4 - Ion velocity [m/s].

In fig (9.3) the electron velocity in the presence of magnetic has increased when compared to no magnetic field. The increment of velocity can be seen right from the beginning ‘z = 0’ at the cathode exit where there is maximum B field. Similar behavior is seen for the ion’s fig (9.4) this is due to the formation of ambipolar electric field

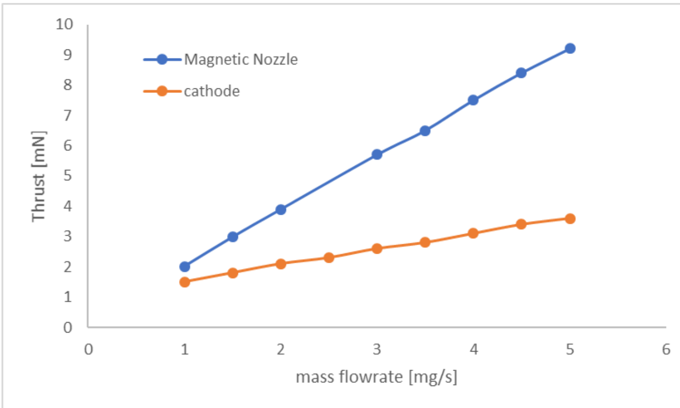

Figure 9.5 - Thrust comparison of cathode with and without magnetic nozzle.

X. Summary and Conclusions

In this work the plasma fluid equations including the magnetic field **B** have been studied and applied for finding the acceleration of plasma in the magnetic nozzle. The initial equations which are in the divergence form have been reduced to one-dimensional equations in the cylindrical coordinate system (r, φ, z) under the assumption that the properties of the plasma do not vary in the radial and azimuthal direction. The model combines the electron, ion and neutral equation of motion and includes 1) the source term in the continuity equation; 2) electron-ion and electron-neutral collisions; 3) the magnetic mirror force; 4) the acceleration of ions due to the formation of the ambipolar electric field.

The numerical integration of the equations yields the expected results. From Figure 9.3 we can see that, as the electrons move into the diverging magnetic field region, the velocity increases when compared to non-magnetized electrons; this confirms that exchange is taking place between parallel and perpendicular kinetic energy. On the other hand, the velocity of the non-magnetized ions (Fig. 9.4) increases as a function of distance. There is a considerable increment in the velocities of the ion when using magnetic nozzle by which we can confirm that the ambipolar electric field is the cause for this increment.

The use of magnetic nozzle for the hollow cathode to accelerate the plasma has increased the performance of the cathode in terms of thrust (Fig. 9.5), which is twice as much with respect to that of a cathode without magnetic nozzle. An experimental verification has to be done to check or compare the obtained theoretical thrust.

Acknowledgments

The author would like to thank Dr. Giulia Becatti and Prof. Fabrizio Paganucci, University of Pisa, without whom this work would not have been possible.

References

1. Frans H. Ebersohn, P. Sheehan and Alec D. Gallimore, "Quasi-one-dimensional particle-in-cell simulation of magnetic nozzles", IEPC-2015-357/ISTS-2015-b-357, 34th International Electric Propulsion Conference and 6th Nano-satellite Symposium Hyogo-Kobe, Japan July 4–10, 2015
2. M. Merino E. Ahedo, "Magnetic nozzle for space plasma thrusters", in Encyclopedia of Plasma Technology 2, edited by J. Leon Shohet, Taylor and Francis, 2016
3. Frans Hendrik Ebersohn, "Kinetic Method for Quasi-One-Dimensional Simulation of Magnetic Nozzle Plasma Dynamics", PhD Thesis Dissertation, Aerospace Engineering, University of Michigan. http://hdl.handle.net/2027.42/133315
4. Daniela Pedrini, Federico Torrini, Jacopo Grassi, Fabrizio Paganucci, "Development of Hollow Cathodes for 5 to 20 kW Hall Thrusters", IEPC-2017-364, Proc. 35th International Electric Propulsion Conference, Atlanta, Georgia, 2017
5. A.N Grubisic and S.B Gabriel, "Thrust production mechanism in hollow cathode micro thrusters", University of Southampton, SO17 1ST, ISBN 978-1-4244-3887-7, 2010. doi: 10.1109/AERO.2010.5446770
6. J.A Bittencourt, "Fundamentals of plasma physics", 3rd edition, Springer International, ISBN 0-387-20975-1
7. Dan M. Goebel and Ira Katz, "Fundamentals of Electric Propulsion", JPL - California Institute of Technology.
8. F. Paganucci, T. Andreussi, "Lecture notes: Electric Propulsion 1", University of Pisa, Italy.